https://doi.org/10.5194/egusphere-2025-676
Preprint. Discussion started: 25 March 2025

The effect of rainfall variability on Nitrogen dynamics in a small agricultural catchment

Qiaoyu Wang[1], Jie Yang[1, 2], Ingo Heidbüchel[3, 4], Teng Xu[1], Chunhui Lu[1,2]

[1]The National Key Laboratory of Water Disaster Prevention, Hohai University, Nanjing, China

[2]College of Hydrology and Water Resources, Hohai University, Nanjing, China

[3]UFZ - Helmholtz-Centre for Environmental Research GmbH, Department of Hydrogeology, Leipzig, Germany

[4]Hydrologic Modeling Unit, Bayreuth Center of Ecology and Environmental Research (BayCEER), University of Bayreuth, Bayreuth, Germany

Correspondence to: Jie Yang (yangj@hhu.edu.cn); Chunhui Lu (clu@hhu.edu.cn)

https://doi.org/10.5194/egusphere-2025-676
Preprint. Discussion started: 25 March 2025

Abstract. Throughout history, extreme storms and droughts have had serious impacts on society and ecosystems globally. Rainfall variability in particular has been identified as a primary performance of climate change. However, so far little has been done to explore the effect of rainfall variability on water quality. This study is aimed at investigating the effect of rainfall variability on nitrogen (N) dynamics and its potentially negative influence on water quality. The transport of water and nitrate was simulated for a small agricultural catchment in Central Germany using the fully coupled surface-subsurface model HydroGeoSphere. Rainfall time series with specific climatic characteristics were generated using a stochastic rainfall generator. N transformation and transport were compared for four scenarios (with high, normal, low annual precipitation amounts, and low annual precipitation amounts coupled with reduced plant uptake, respectively) in order to identify the impact of inter-annual rainfall variability on N dynamics. The results suggest that higher annual precipitation amounts can enhance the transformation and transport of nitrogen. Lower annual precipitation amounts are conducive to nitrogen retention. Nonetheless, when vegetation suffers from drought stress, the retention capacity will decline markedly, suggesting that vegetation plays a vital role in N dynamics under extreme droughts. The linear regressions between selected parameters of the rainfall generator and N loads / fluxes were analyzed to elucidate the impact of intra-annual rainfall variability on N dynamics. The results indicate that wet / dry conditions and different dry-wet patterns caused by the distribution of storm durations and inter-storm periods over the course of a year can significantly affect N loads and in-stream nitrate concentration, respectively. In the warm season, droughts prompt the accumulation of SON, but drying-wetting cycles can enhance the extensive transformation of SON. In-stream nitrate concentration dramatically elevates during the rewetting period after the drought. High mean rainfall intensity contributes not only to the transformation of N when mineralization is not limited by low temperatures, but also to the plant absorption of inorganic nitrogen in the growing season. There is merely small effect of mean rainfall intensity on stream water quality. Overall, the study clarifies the effect of rainfall variability on N dynamics in a small agricultural catchment, which provides theoretical support to formulate fertilization strategies and protect aquatic ecosystems under climate change in the future.

Key Points: N dynamics, HydroGeoSphere, Rainfall variability, Stochastic rainfall generator

https://doi.org/10.5194/egusphere-2025-676
Preprint. Discussion started: 25 March 2025

1 Introduction

In the past decades, extreme climate events intensified by human-induced climate change have frequently occurred globally [Pall et al., 2011; Min et al., 2011; Williams et al., 2015; Hari et al., 2020] and caused socioeconomics, natural ecosystems, and crop cultivation to suffer severely [European Commission, 2006; Wegren et al., 2011; Van Lanen et al., 2016; BDF, 2019; Markonis et al., 2021; Black, 2023]. The hydrological processes are susceptible to meteorological conditions on various spatial and temporal scales [Ionita et al., 2017; Laaha et al., 2017; Zhang et al., 2021]. Most extreme climate events tend to cause water scarcity and poor water quality at regional scales [Zwolsman and van Bokhoven, 2007; Delpla et al., 2009; Whitehead et al., 2009; Stahl et al., 2016; Ballard et al., 2019; Bauwe et al., 2020; Geris et al., 2022]. Under future global warming scenarios, a higher frequency and intensification of extreme climate events from daily to multiyear timescales will occur [O'Gorman et al., 2009; Dai et al., 2013; Fischer and Knutti, 2014; Spinoni et al., 2018; Hari et al., 2020; Zhang et al., 2024]. Thus, their effect on water resources has attracted much attention around the world.

Heavy rainstorms and severe droughts being the predominant extreme climate events around the globe share the common characteristic of rainfall variability [Trenberth et al., 2011; Pendergrass et al., 2017; Hanel et al., 2018]. During heavy rainstorms, extraordinary rainfall amounts and intensities cause large amounts of rainwater to infiltrate into soils and trigger flash floods in a short time. Increased groundwater flow

https://doi.org/10.5194/egusphere-2025-676
Preprint. Discussion started: 25 March 2025

and enhanced surface runoff stimulate the movement of solutes retained in the soil, which thereby can lead to water quality degradation [Geris et al., 2022]. Different from heavy rainstorms, severe droughts driven by precipitation deficits need to take several months or potentially years to reach their full intensity [Otkin et al. 2018], from which it takes 1-2 years for hydrological components to recover [Hanel et al., 2018]. Wilusz et al. [2017] decomposed the relationship between rainfall variability and transit times, a reflection of water velocities that control solute transport, and illustrated that climate change may seasonally alter the ages of water in streams and thereby influence water quality in the future. Nitrate (NO_3^--N) is the major solute threatening the quality of drinking water and destroying the structure and functions of aquatic ecosystems [Vitousek et al., 2009; Alvarez-Cobelas et al., 2008; Dupas et al., 2017]. The nitrate turnover processes established at the catchment scale are expected to change due to climate change [Whitehead et al., 2009; Hesse and Krysanova, 2016; Mosley, 2015], especially due to increasing drought events [Zwolsman and van Bokhoven, 2007; Ballard et al., 2019; Zhou et al., 2022; Winter et al., 2023].

Several extreme climate events (extreme rainfall and droughts) occurred in Central Europe during the last two decades, which has attracted worldwide attention. Extreme rainfall in 2002, 2013, and 2021 cause a threat to humans and large damages to the environment, economy, and infrastructure [Ulbrich et al., 2003; Thieken et al., 2016; Voit, P. and Heistermann, M., 2024]. Three remarkable summer droughts occurred in

https://doi.org/10.5194/egusphere-2025-676
Preprint. Discussion started: 25 March 2025

2003, 2015, and 2018–2019 (consecutive), driven by precipitation deficit in conjunction with temperature anomalies during the vegetation growing period [Fink et al., 2004; Schär et al., 2004; Ciais et al., 2005; Orth, Vogel, Luterbacher, Pfister, & Seneviratne, 2016; Hanel et al., 2018; Hari et al., 2020; Camenisch et al., 2020], of which the 2018 event caused unprecedented tree mortality in many species throughout the Central European forests and unexpectedly strong drought-legacy effects [Schuldt et al., 2020]. Zhou et al. [2022] detected higher soil N surplus (total N input with the crop/plant uptake subtracted) and decreased the terrestrial N export in agricultural areas located in Central Germany during the drought years (2015-2018). The same phenomenon reported in the Nitrate Report 2020 of the Netherlands (RIVM, 2021) indicates that more N was retained in the soil during the drought period compared to the pre-drought period. However, by studying the 2018–2019 (consecutive) drought in Central Germany, Winter et al. [2023] drew the conclusion that severe multi-year droughts can reduce the nitrogen (N) retention capacity of catchments. It seems that the opposite conclusions drawn from these studies can be attributed to the different investigation timescales. The latter study considering the subsequent rewetting period during which most nitrogen accumulated during the drought left the catchment. Leitner et al. [2020] also found that in the year after a summer drought, NO_3^- leaching via soil water seepage was significantly elevated compared to the long-term mean in a temperate mixed forest on karst, an observation which was made in wetland-influenced catchments as well [Watmough et al., 2004]. These prove that rainfall variability has a

https://doi.org/10.5194/egusphere-2025-676
Preprint. Discussion started: 25 March 2025

profound impact on N dynamics. Therefore, it's imperative to shed light on the impact of rainfall variability on water quality in terms of N dynamics.

A small agricultural catchment in Central Germany was selected as the study site, where a hydrological model was previously established utilizing the fully coupled surface-subsurface numerical simulator HydroGeoSphere [Yang et al., 2018]. The framework of N dynamics was modified from the ELEMeNT approach [Yang et al., 2021]. Rainfall time series with specific climatic characteristics were generated using a stochastic rainfall generator [Robinson & Sivapalan, 1997] to take the place of the rainfall data in the simulation period. The work is divided into two main components. First, we explored the influence of inter-annual rainfall variability. Three representative years (with high, normal, and low annual precipitation amounts, respectively) were chosen from the past two decades in Central Germany as the target scenarios. A fourth scenario with low annual precipitation amounts coupled with reduced plant uptake represents the situation that vegetation is partially destroyed by extreme droughts. The statistical analyses of nitrogen loads and fluxes and a comparison across different scenarios were conducted. Second, we explored the impact of intra-annual rainfall variability. By separately altering specific parameters, rainfall time series were generated by the stochastic rainfall generator. Using these rainfall data, the flow and nitrogen transport were simulated across hundreds of models. The responses of the N loads and fluxes to the parameters (e.g., the amplitudes of the seasonal variations in the storm durations

https://doi.org/10.5194/egusphere-2025-676
Preprint. Discussion started: 25 March 2025

and inter-storm period) were thoroughly analyzed subsequently.

2 Data collection

2.1 Study Site

The studied catchment, Schäfertal, is located on the lower reaches of the eastern Harz Mountains, Central Germany, with an area of 1.44 km^2. Since 1968, this first-order catchment has been subject to broad hydrogeological investigations, analyses, and research [Altermann et al., 1970; Altermann et al., 1977; Borchardt et al., 1981; Altermann et al., 1994; Wollschläger et al., 2016]. The valley bottom contains riparian zones with pasture and a small channel (Figure 1a). The hillslopes on both sides of the channel have an average slope of 11°, mostly used as farmland. The farmland undergoes intensive agriculture, primarily winter wheat growing [Yang et al., 2018]. Two small portions near the western edge are mostly forest. The types of land use in the catchment do not generally convert until the economic and ecological goals vary between years, e.g., shifting between planting and pasture [Wang et al., 2023]. A meteorological station, which is 200 m from the catchment outlet, provides records of precipitation, air and soil temperatures, radiation, and wind speed. The catchment outlet in the stream, where a gauge station was built, is considered as the unique exit that allows water and solute to leave the catchment and enter the downstream catchments. This is because a subsurface wall (~55 m long and ~7 m deep) was erected across the valley to block subsurface flow. The gauge station provides discharge data at 10-minute intervals, aggregated to

https://doi.org/10.5194/egusphere-2025-676
Preprint. Discussion started: 25 March 2025

daily means in this study. Nitrate concentration data is measured by sampling near the gauge station.

The aquifer is thin, with the thickness varying from ~5 m near the valley bottom to ~2 m at the top of the hillslopes (Figure 1a). Thirteen wells, each ~2 meters deep, were constructed and fitted with automated data loggers to record groundwater levels. The groundwater levels exhibit pronounced seasonal variations, rising to the land surface during winter and receding to depths of ~3 meters below the ground during summer. The groundwater storage is low (~500 mm, stored water volume divided by catchment area). Most of the groundwater converges towards the channel vicinity, with the upper sections of the hillslopes typically in an unsaturated state [Yang et al., 2018]. Luvisols and Gleyic Cambisols are the aquifer materials of the hillslope. The valley bottom is dominated by Gleysols and Fluvisols (Figure 1b) [Anis and Rode, 2015]. Generally, the aquifer is comprised of two horizontal layers: a top layer of approximately 0.5 m thickness, with higher permeability, higher porosity, and the developed root zone from crops; and a base layer with less permeability due to the high loam content [Yang et al., 2018]. The bedrock underlying the aquifer comprises greywacke and shale [Graeff et al., 2009]. Owing to the aquifer material and unknown hydraulic properties, the bedrock is often regarded as impermeable.

https://doi.org/10.5194/egusphere-2025-676
Preprint. Discussion started: 25 March 2025

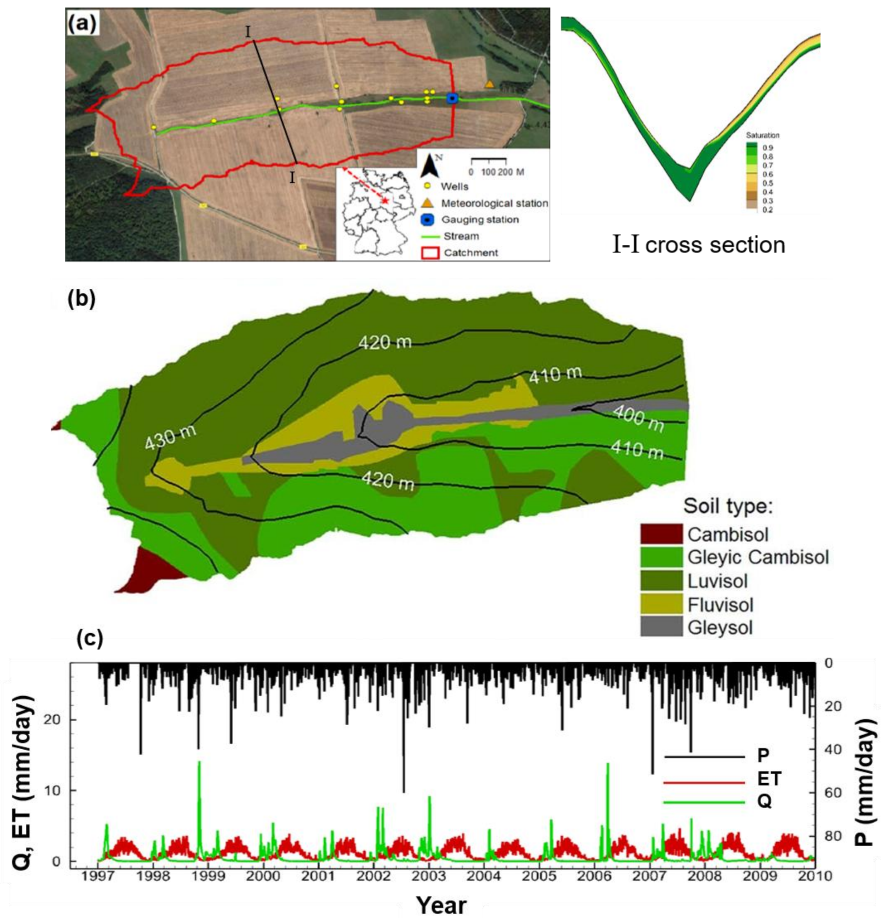

Figure 1. (a) The catchment 'Schäfertal' is located in Central Germany (background image from © Google Maps). The red line indicates the dividing ridge of the catchment [*Anis* and *Rode*, 2015]. I-I cross section shows the aquifer thickness variation. (b) The distribution of soil type in the catchment. (c) The measured daily precipitation (P), discharge (Q), and the simulated actual evapotranspiration (ET) [*Yang et al*., 2018].

2.2 Measured data

The studied catchment exhibits a temperate and humid climate with pronounced seasonality. The humid climate in wet regions is quantified by an aridity index of 1.0. The ET is the main driver of the hydrologic seasonality, as the precipitation is uniformly

https://doi.org/10.5194/egusphere-2025-676
Preprint. Discussion started: 25 March 2025

distributed across the year. According to the meteorological data records from 1997 to 2010, the mean annual precipitation (P) and discharge (Q) are 610 mm and 160 mm, respectively (Figure 1c). Based on the 14-year water balance (P = ET + Q), the actual mean annual evapotranspiration (ET) is 450 mm. The in-stream nitrate concentration (C_Q) was measured at fortnightly to monthly intervals [Dupas et al., 2017], covering the period 2001-2010. The N surplus, which is the annual amount of nitrogen remaining in the soil after the consumption by plant uptake from the external N input, was estimated as 48.8 kg N ha^{-1} $year^{-1}$ during 1997–2010 for this catchment [Bach and Frede, 1998; Bach et al., 2011]. Adequate data from numerous investigations and previous research supports the exploration of N dynamics in the agricultural catchment.

3 Methodology

The hydrological model for the Schäfertal catchment was established using HydroGeoSphere [Therrien et al., 2010] in the previous study [Yang et al., 2018]. The framework of N dynamics [Yang et al., 2021] modified from the ELEMeNT modeling approach [Exploration of Long-tErM Nutrient Trajectories, Van Meter et al., 2017] was applied to track the fate of N in soil and groundwater in the present study. In order to investigate the effect of rainfall variability on N dynamics, rainfall time series, substituting for the precipitation data during the simulation period, were generated by a stochastic rainfall generator [Robinson & Sivapalan, 1997; Wilusz et al., 2017]. These models are described below in details.

https://doi.org/10.5194/egusphere-2025-676
Preprint. Discussion started: 25 March 2025

3.1 Flow modelling

HydroGeoSphere is a 3D control volume finite element simulator that can model fully coupled surface-subsurface hydrological processes by the dual nodes approach. It can not only describe crucial hydrological processes such as dynamical evapotranspiration, snow, sublimation, snowmelt, and freeze and melt of pore water, but also simulate 2D overland flow by Manning's equation and the diffusive-wave approximation of the St. Venant equations, 3D variably saturated underground flow by Richards' equation and Darcy's law, flow in porous media, as well as the transport of reactive solutes. In addition, HydroGeoSphere allows the simulation of 1D surface flow in a channel network and water exchange flux between the channel domain and the subsurface domain [Yang et al., 2015]. HydroGeoSphere has been frequently used to model catchment hydrological processes and solute transport in many previous studies [e.g., Therrien et al., 2010; Yang et al., 2018]. Please refer to Therrien et al. [2010] for the governing equations and technical details.

The hydrological model of Schäfertal catchment is briefly recapitulated in the following. More details are provided in Yang et al. [2018]. In the model, the subsurface domain between the surface and bedrock was depicted using 3D prisms with side length ranging from 30 m to 50 m. The surface domain was filled by the uppermost 2D triangles of the generated 3D prismatic mesh, while the channel was delineated by 1D segments with specified widths and depths. According to different aquifer materials and the difference

https://doi.org/10.5194/egusphere-2025-676
Preprint. Discussion started: 25 March 2025

in their permeability in the vertical direction, the subsurface domain was separated into ten property zones with zonal hydraulic conductivity and porosity values. The surface domain and channel were parameterized with a Manning roughness coefficient representing the land use. Spatially uniform and temporally variable precipitation (Figure 1c) was applied to the entire surface domain. ET is computed as a combination of plant transpiration from the root zone and evaporation down to the evaporation depth [Therrien et al., 2010]. A critical depth boundary condition was assigned to the outlet in the channel domain to simulate the discharge (Q) of the catchment. In order to eliminate the influence of initial conditions, a preliminary model run was performed for the period spanning 1997 to 2007. The simulated results at the end of the period were taken as initial conditions for the actual simulations.

Key parameters that significantly influence the hydrological processes were selected for the calibration [Anis & Rode, 2015; Graeff et al., 2009] using the software package PEST [Doherty & Hunt, 2010]. PEST uses the Marquardt method to minimize a target function by varying the values of a given set of parameters until the optimization criterion is reached. The groundwater levels measured in groundwater wells and the discharge measured at the gauging station were used as target variables. Considering high CPU time (~1 day to run the model for the period for 14 year), the calibration period spans 1 year, from October 2002 to October 2003. Subsequently, the calibrated model was verified over the entire simulation period.

https://doi.org/10.5194/egusphere-2025-676
Preprint. Discussion started: 25 March 2025

3.2 Nitrogen transport in soil and groundwater

The transformation and transport of nitrogen in the underground area are tracked by the framework of N dynamics modified from ELEMeNT. ELEMeNT is a comprehensive model maintaining a landscape memory, that is, considering the effect of not only current conditions but also past land use and nutrient dynamics on current fluxes [Van Meter et al., 2017]. The modification includes four parts in the framework. Firstly, the N surplus is estimated by subtracting the plant uptake from external N input [Yang et al., 2021]. Secondly, plant uptake was delineated corresponding to the reality. Thirdly, denitrification was considered in both the N source zone in soil and groundwater. Lastly, the process of transferring nitrogen from the source zone to groundwater was delineated by leaching.

External nitrogen input goes through transformation and transport in the soil, subsequently filters into groundwater and gets exported to the surface water body. In route, every kind of nitrogen undergoes biogeochemical processes. The framework includes a N source zone forming in shallow soil and a groundwater zone (Figure 2). There are two assumptions in the N source zone: 1) the total N load in the N source zone is comprised of an organic N (SON) pool and an inorganic N (SIN) pool; 2) the external N input contributes only to the SON. The external N input represents atmospheric deposition, biological fixation, animal manure from the pasture area, and N fertilizer from the farmland. The SON is further distinguished as active SON with

https://doi.org/10.5194/egusphere-2025-676
Preprint. Discussion started: 25 March 2025

faster reaction kinetics and protected SON with slower reaction kinetics. Both SON(a) and SON(p) are transformed into SIN by mineralization. SIN is further consumed by plant uptake and denitrification, and leaches from soil to groundwater as dissolved inorganic N (DIN), representing mainly nitrate in the studied catchment [Yang et al., 2018; Nguyen et al., 2021]. DIN can further undergo denitrification until being exported to the stream. The framework is considered to be acceptable based on the fact that most of the nitrate fluxes undergo biogeochemical transformation in the inorganic N pool [Haag and Kaupenjohann, 2001].

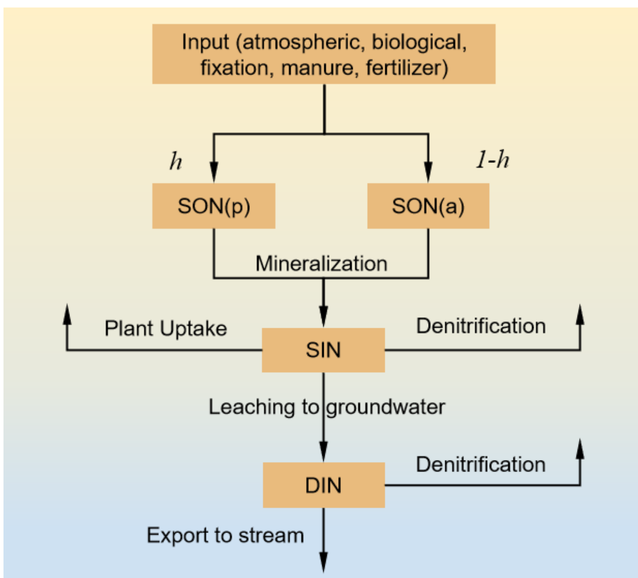

Figure 2. The framework simulating the Nitrogen Transport in soil and groundwater, modified based on [Yang et al., 2021].

The governing equations to calculate N fluxes follow the ones of the framework in Yang et al. [2021]. The land-use dependent protection coefficient *h* [Van Meter et al., 2017] determines the amount of external N input that contributes to the protected SON

https://doi.org/10.5194/egusphere-2025-676
Preprint. Discussion started: 25 March 2025

(SON(p)), and the residual contributes to the active SON (SON(a)). Mineralization and denitrification are described as first-order processes. Based on the results of Wang et al. [2023], the effect of wetness is considered in mineralization, using:

$$MINE_a = k_a \cdot f(temp) \cdot f(wetness) \cdot SON_a \quad (1)$$

$$MINE_p = k_p \cdot f(temp) \cdot f(wetness) \cdot SON_p \quad (2)$$

$$DENI_s = \lambda_s \cdot SIN \quad (3)$$

$$DENI_g = \lambda_g \cdot DIN \quad (4)$$

where $MINE_a$, $MINE_p$ (kg ha^{-1} day^{-1}) are the mineralization rates for active SON and protected SON, respectively. $DENI_s$ and $DENI_g$ (kg ha^{-1} day^{-1}) are the denitrification rates for SIN and DIN, respectively. k_a, k_p, and λ (day^{-1}) are coefficients for the three first-order processes. $f(temp)$ and $f(wetness)$ are factors representing the constraints by soil temperature and wetness [Lindström et al., 2010; Wang et al., 2023], respectively. Plant uptake rate UPT follows the equation used in the HYPE model [Lindström et al., 2010]:

$$UPT = min\,(UPT_P, 0.8 \cdot SIN) \quad (5)$$

$$UPT_P = p1/p3 \cdot (\frac{p1-p2}{p2}) \cdot e^{-(DNO-p4)/p3} / (1 + (\frac{p1-p2}{p2}) \cdot e^{-(DNO-p4)/p3})^2 \quad (6)$$

where UPT and UPT_P (kg ha^{-1} day^{-1}) are the actual and potential uptake rates, respectively. The logistic plant growth function is considered in the equation of potential uptake rates. DNO is the day number within a year. *p1*, *p2*, *p3* are three

https://doi.org/10.5194/egusphere-2025-676
Preprint. Discussion started: 25 March 2025

parameters depending on the type of plants, whose units are (kg ha^{-1}), (kg ha^{-1}), and (day), respectively. *p4* is the day number of the sowing date. The leaching rate adapts a first-order process considering soil saturation and groundwater velocity, using:

$$LEA = k_l \cdot f_w \cdot f_q \cdot SIN \quad (7)$$

$$f_w = \frac{S - S_r}{1 - S_r} \quad (8)$$

$$f_q = MIN(\frac{q}{q_{ref}}, 1) \quad (9)$$

where LEA is the leaching flux of SIN from the N source zone to the groundwater, k_l is a leaching coefficient (day^{-1}), f_w and f_q are two factors representing the constraints of soil saturation and groundwater velocity to the leaching process, respectively. S is the soil saturation, and S_r is the residual saturation. q (m day^{-1}) is the groundwater Darcy flow rate, q_{ref} (m day^{-1}) is a reference Darcy flow rate. This formulation of LEA is modified from the one used in Van Meter et al. [2017].

In these hydrogeochemical processes, a portion of N is retained in the catchment as the biogeochemical legacy in soil or the hydrological legacy in groundwater or permanently leaves catchments by denitrification, which does not degrade the water quality of the catchment during a certain period. Therefore, the N retention is used to quantify a catchment's capacity to prevent nitrogen from entering surface water bodies during a certain period [Wang et al., 2023], which is the fraction of the N retained in the catchment and consumed via denitrification to the total external N input, calculated using [*Ehrhardt et al*., 2021]:

https://doi.org/10.5194/egusphere-2025-676
Preprint. Discussion started: 25 March 2025

$$\text{Retention} = 1 - \frac{N_{out}}{N_{in}} = 1 - \frac{\int_{t_1}^{t_2} N_{outlet}}{\int_{t_1}^{t_2} N_{input}} \tag{3}$$

where the N_{outlet} is the N mass leaving the catchment through the outlet during the time period $(t_1 - t_2)$.

Due to the lack of spatiotemporal variation information of the external N input, its value was fixed at 180 kg ha^{-1} year^{-1} according to Nguyen et al. [2021], where the N balance was simulated in the upper Selke catchment covering the Schäfertal catchment. The protection coefficient h was selected as 0.3 according to the values reported in Van Meter et al. [2017]. $p4$ as the sowing date of plant growth activities was set to 63 days (early March) [Yang et al., 2018]. The DIN was transported in the coupled surface water-groundwater system, with longitudinal and transverse dispersion coefficients of 8 and 0.8 m, respectively. Other parameters relative to N dynamics were calibrated by PEST in empirical ranges. The measured C_Q at the gauge station and the N surplus of 48.8 kg N ha^{-1} year^{-1} were used as the target variables. The calibration period spans from March 2001 to August 2003, during which successive C_Q data was obtained. The CPU time was ~2 h for a single iteration. The model validation was conducted over the entire simulation period from 1997 to 2010 (~1 day of CPU time). The calibrated best-fit values for the transport parameters are listed in Table S1 [see in Supporting Information]. For more details refer to Wang et al. [2023].

The N source zone serves as a boundary condition at the top of the aquifer for simulating DIN transport in the groundwater. The bedrock is treated as impermeable for nitrate.

https://doi.org/10.5194/egusphere-2025-676
Preprint. Discussion started: 25 March 2025

The catchment outlet is the only boundary allowing the exit of nitrate from the catchment. In order to minimize the influence of the initial conditions, a preliminary transport simulation (together with the flow simulation) was performed with zero load in the SON and SIN pools and zero DIN concentration in the catchment, such that a quasi-steady state for the SON and SIN pools can be reached at the end of the preliminary simulation. The resulting data (N loads and concentrations) were used as initial conditions for the actual simulations.

3.3 Stochastic rainfall generator

In order to investigate the effect of rainfall variability on N dynamics, rainfall time series with different climatic characteristics were generated by a stochastic rainfall generator. The stochastic rainfall generator is stochastic model of rainfall time series originally created to investigate the timescales of flood frequency response to rainfall, incorporating any combinations of storm, within-storm as well as between-storm, and seasonal variabilities of rainfall intensity [Robinson & Sivapalan, 1997]. It can exhibit a good performance of rainfall variability under climate change [Wilusz et al., 2017]. The identification of individual storms is based on the criterion of a specified minimum dry period between events. Acreman [1990] noted the arbitrary nature of this criterion in the selection of the minimum dry period. In this study, the minimum dry period was set at 1 day (24 hours) due to the daily average meteorological data, which is consistent with Wilusz et al. [2017].

https://doi.org/10.5194/egusphere-2025-676
Preprint. Discussion started: 25 March 2025

The rainfall generator generates daily rainfall time series meeting the research requirement in three steps. First, determine a series of alternating storm durations t_r and inter-storm periods t_b over the simulation time that are independent of each other and vary seasonally. Second, determine the average rainfall intensity i of each storm. It is described as a random variable stochastically dependent on storm duration t_r. Third, construct within-storm rainfall intensity variations using a normalized mass curve [Huff, 1967; Chow et al., 1988]. The detailed governing equations can be found in Sect. S1 of the Supporting Information.

We adopted the source code in Python v2.7 of the rainfall generator from Wilusz et al. [2017]. In the stochastic model, the seasonal averages (γ_s and δ_s), amplitudes (α_γ and α_δ), and phases (τ_γ and τ_δ) are used to determine monthly average storm duration and inter-storm period. a_1^1~a_1^4, b_1^1~b_1^4, a_2 and b_2 are the parameters characterizing the dependence between average rainfall intensity and storm duration for the four seasons (the first season (Jan - Mar), the second season (Apr - June), the third season (Jul - Sep), and the fourth season (Oct - Dec)). In addition, there is an isolated parameter $P_{drizzle}$ in the source code, a threshold of the identifiable storm. The storms with precipitation greater than $P_{drizzle}$ can be identified as synoptic frontal events.

Rainfall time series representing different climate conditions were generated following these steps below:

(i) Three representative years were selected according to historical meteorological data, which are the wet year 2007 (P = 916.3 mm), the normal

https://doi.org/10.5194/egusphere-2025-676
Preprint. Discussion started: 25 March 2025

year 2008 (P = 588.7 mm), and the dry year 2018 (P = 444.1 mm);

(ii) For each of the representative years, a set of parameters was determined so that the generated rainfall time series can fit the actual rainfall data of this year best. This inverse process was conducted using PEST;

(iii) The three sets of best-fit parameters (Table 1) were used again to generate 100 stochastic realizations (rainfall time series), for the wet, normal and dry year, respectively. These realizations may deviate from the actual rainfall data in terms of daily rainfall values, still being statistically identical with the rainfall pattern of the representative years.

https://doi.org/10.5194/egusphere-2025-676
Preprint. Discussion started: 25 March 2025

Table 1. Three parameter sets of the rainfall generator, for the wet, normal and dry year, respectively.

Parameter	Wet Year (2007)	Normal Year (2008)	Dry Year (2018)	Adjustable range	Note
P(mm)	916.3	588.7	444.1	(400,1000)	Annual precipitation
γ_s(day)	2.546	2.177	2.071	(0.1, 10)	Seasonally averaged storm duration
δ_s(day)	7.988	7.424	7.535	(0.1, 10)	Seasonally averaged inter-storm period
α_γ(day)	1.764	0.820	0.550	(-2.2, 2.2)	Amplitude of seasonal storm shift
α_δ(day)	2.457	2.962	2.946	(-8, 8)	Amplitude of seasonal inter-storm shift
$(a_1, b_1)_1$	(0.875, 2.349)	(0.934, 1.802)	(0.909, 1.598)	(0.1, 5)	Coefficient 1 and 2 of the first season (Jan-Mar) for expected storm intensity
$(a_1, b_1)_2$	(1.015, 0.661)	(0.894, 0.538)	(0.857, 0.456)	(0.1, 5)	Coefficient 1 and 2 of the second season (Apr-Jun) for expected storm intensity
$(a_1, b_1)_3$	(0.917, 1.121)	(0.968, 0.845)	(0.947, 0.752)	(0.1, 5)	Coefficient 1 and 2 of the third season (Jul-Sep) for expected storm intensity
$(a_1, b_1)_4$	(1.666, 1.556)	(1.348, 1.341)	(1.392, 1.263)	(0.1, 5)	Coefficient 1 and 2 of the fourth season (Oct-Dec) for expected storm intensity
(a_2, b_2)	(0.658, 0.961)	(0.617, 1.057)	(0.632, 1.025)	(0.1, 5)	Coefficient 1 and 2 for expected storm variability
$P_{drizzle}$	0.137	0.146	0.140	(0.01, 0.99)	Probability of drizzle event
τ_γ(day)	105.760	100.297	100.474	/	Phase of seasonal storm shifts
τ_δ(day)	120.665	124.044	124.161	/	Phase of seasonal inter-storm shifts

https://doi.org/10.5194/egusphere-2025-676
Preprint. Discussion started: 25 March 2025

3.4 Simulation scenarios

3.4.1 Inter-annual rainfall variability

Wet Year (WY), Normal Year (NY), and Dry Year (DY) were set as the simulation scenarios. In addition, a fourth scenario being similar to the Dry Year but coupled with reduced plant uptake was considered as Extreme Dry Year (EDY). This EDY scenario was used to account for the extreme drought occurring in 2018 that caused vegetation to die back with lower plant uptake and impacted N dynamics to some extent [Winter et al., 2023]. In the EDY scenario, the plant uptake was assumed to decrease down to 36% of the original value used in the DY scenario, according to the classification and the occurrence period of the drought [Liu et al., 2010]. For each of the scenarios, the water flow and N transport model was conducted 100 times by substituting the rainfall data during the simulation period with the generated 100 stochastic rainfall time series (Figure S1 in Supporting Information). Average annual N loads and fluxes under each scenario can be calculated to ensure that they were not controlled by a single realization and statistically meaningful. Additionally, we simulated the fluctuations of C_Q in each scenario with time over three years. Finally, the average annual N loads, fluxes, and C_Q as well as the variation of C_Q can be cross-compared and analyzed to elucidate the effect of inter-annual rainfall variability on N dynamics.

3.4.2 Intra-annual rainfall variability

In order to explore the effect of intra-annual rainfall variability on N dynamics, the

https://doi.org/10.5194/egusphere-2025-676
Preprint. Discussion started: 25 March 2025

linear regression analyses between the parameters of the stochastic rainfall generator and N loads, fluxes as well as C_Q were conducted based on the Normal Year (2008). The seasonal averages of storm duration and inter-storm period (γ_s and δ_s), the amplitudes of the seasonal variations in storm duration and inter-storm period (α_γ and α_δ), the average rainfall intensity of four seasons (E_1~E_4) and squared coefficient of variation of the average rainfall intensity (CV^2), as well as the probability of drizzle event ($P_{drizzle}$), were selected as the experimental parameters. E_1~E_4 and CV^2 can be approximately calculated by equation S5 & S6, using relative parameters and seasonally averaged storm duration (γ_s). In total, 15 parameters (Table 1) were subjected to the assessment of their effect on N dynamics.

For each of the experimental parameters, the rainfall generator generated 100 rainfall time series randomly, whose annual precipitations are within the historical range, with this experimental parameter varying randomly within the adjustable range but other parameters being fixed to the best-fit values for the Normal Year. The ranges of the experimental parameters used in the linear regression analyses are listed in Table 1. Finally, the response of the average annual N loads, fluxes and C_Q to different rainfall parameters can be analyzed.

https://doi.org/10.5194/egusphere-2025-676
Preprint. Discussion started: 25 March 2025

4 Results

4.1 Effect of Inter-annual rainfall variability

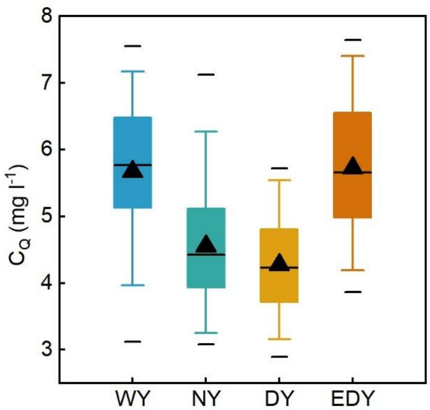

Figure 3. The simulated in-stream nitrate concentration (C_Q) for the scenarios of WY, NY, DY, and EDY. The whisker represents the concentration ranges from 5th to 95th percentiles, with the triangles indicating the median and the lines marking the maximum, average, and minimum of the data set from top to bottom. The same as below.

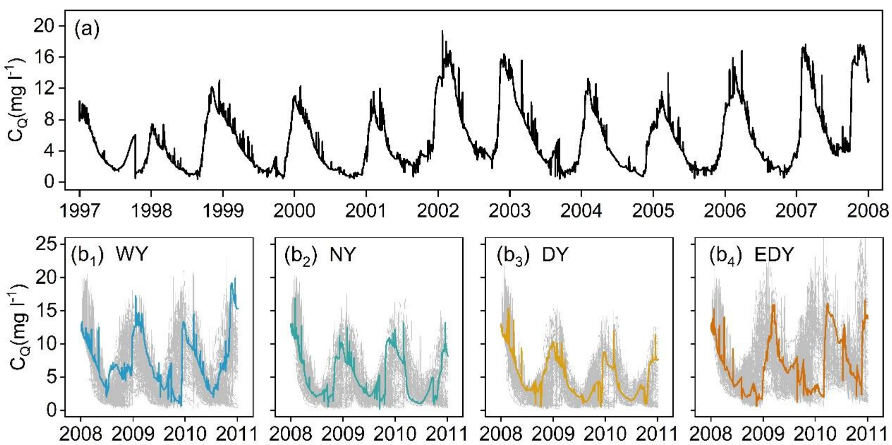

Figure 4. The fluctuations of simulated in-stream nitrate concentration (C_Q) under (a) the historical rainfall (1997-2007) and the scenarios of (b$_1$) WY, (b$_2$) NY, (b$_3$) DY, and (b$_4$) EDY (2008-2010). The grey areas are the simulation uncertainty generated by the acceptable realizations.

Figure 3 shows the simulated in-stream nitrate concentration for the four scenarios. WY

https://doi.org/10.5194/egusphere-2025-676
Preprint. Discussion started: 25 March 2025

produces high C_Q, with the median concentration almost being up to 6 mg l^{-1}. The concentrations generally decrease when the rainfall pattern transforms from WY, via NY, to DY. However, in EDY, when vegetation dying back occurs, concentrations as high as the ones produced in WY can be observed again. The variations of C_Q in these scenarios are exhibited in Figure 4(b_1) ~ (b_4). The range of C_Q generally decreases when the rainfall pattern transforms from WY, via NY, to DY. But, the range of EDY is wider than that of DY, and even similar with that of WY. These results generally suggest that low C_Q are produced in dry years, but high concentrations can be produced in both wet and extreme dry years.

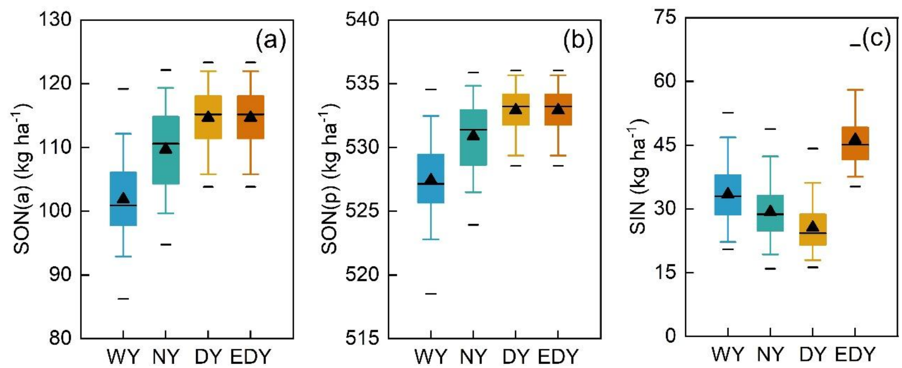

Figure 5. The simulated loads of (a) active soil organic nitrogen (SON(a)), (b) protected soil organic nitrogen (SON(p)), and (c) soil inorganic nitrogen (SIN) for the scenarios of WY, NY, DY, and EDY.

The soil organic nitrogen (SON) loads increase when the rainfall pattern turns from WY, via NY, to DY/EDY (Figure 5a & b). The SON loads in DY and EDY are identical because the vegetation dying back in EDY is not able to influence the transformation of SON. The soil inorganic nitrogen load (SIN) is generally high in WY and low in DY

https://doi.org/10.5194/egusphere-2025-676
Preprint. Discussion started: 25 March 2025

(Figure 5c). However, when vegetation dying back causes reduced plant uptake in EDY, the SIN load can accumulate significantly to the highest level among the four scenarios.

The highest and the lowest N mineralization fluxes are produced in WY and DY, respectively (Figure 6a). DY and EDY have the identical mineralization fluxes. It can be attributed to the lower soil moisture content caused by decreased precipitation constraining the mineralization process. Note that the fluxes of plant uptake, denitrification, and leaching are negative values representing the sink term for the SIN pool. For the plant uptake, the highest N fluxes are produced in WY (Figure 6b). Plant uptake decreases when the rainfall pattern transforms from WY, via NY, to DY, induced by the decreasing soil moisture. In EDY, due to vegetation dying back, plant uptake significantly reduces to the lowest level. The fluxes of denitrification (in soil and groundwater) and leaching (from soil to groundwater) both exhibit decreasing trends when the rainfall pattern transforms from WY, via NY, to DY (Figure 6c & d). It can be explained by the decreasing soil moisture inhibiting the biogeochemical activities, as well as the N mobilization from soil to groundwater. However, for the EDY scenario, large denitrification and leaching fluxes can still be observed even when soil moisture content is small. This is because the plant uptake is significantly constrained in EDY, such that more SIN is available for either consumption via denitrification or leaching into groundwater. The N export flux to the stream generally follows the same patterns as the leaching, with the relatively higher fluxes occurring in WY and EDY and lower fluxes in NY and DY (Figure 6e). It demonstrates that in the catchment, leaching is a

https://doi.org/10.5194/egusphere-2025-676
Preprint. Discussion started: 25 March 2025

key factor to determine the N export from groundwater to stream water.

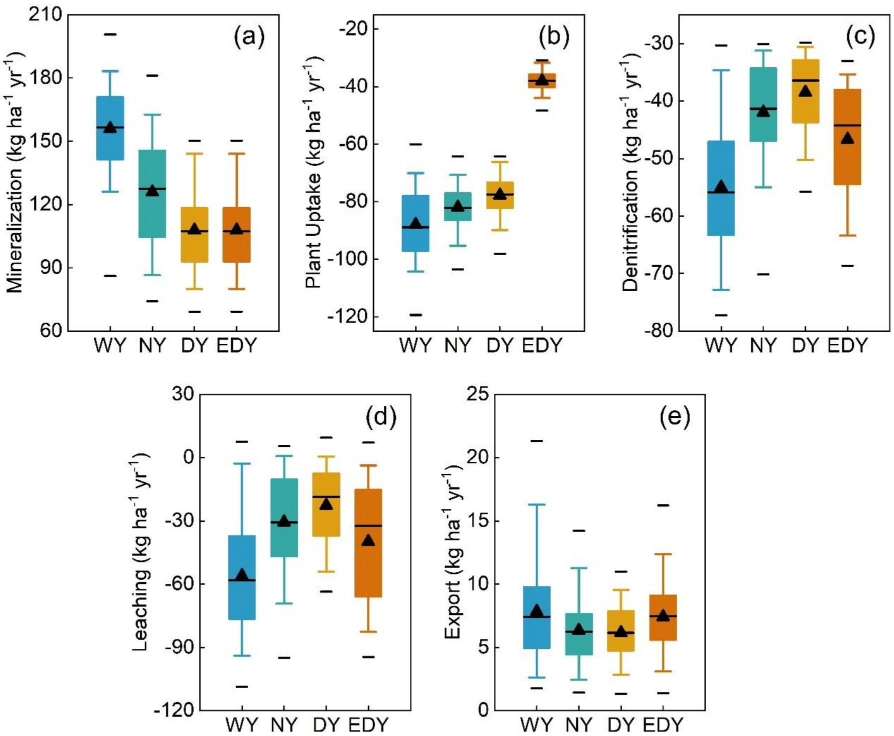

Figure 6. The simulated fluxes of (a) mineralization, (b) plant uptake, (c) denitrification (in soil and groundwater), (d) leaching, and (e) export for the scenarios of WY, NY, DY, and EDY.

4.2 Effect of Intra-annual rainfall variability

The determination coefficients (R^2) of the linear regressions between the parameters of the rainfall generator and the C_Q / N loads / fluxes are illustrated in Figure 7a. Lager R^2 values can be observed for the amplitude of the seasonal variations in the storm duration and inter-storm period (α_γ & α_δ), the average rainfall intensity of the second season and third season (E_2 & E_3). These parameters are the four most important parameters (Figure 7b) that may influence N loads / fluxes, and are subjected to further discussion.

https://doi.org/10.5194/egusphere-2025-676
Preprint. Discussion started: 25 March 2025

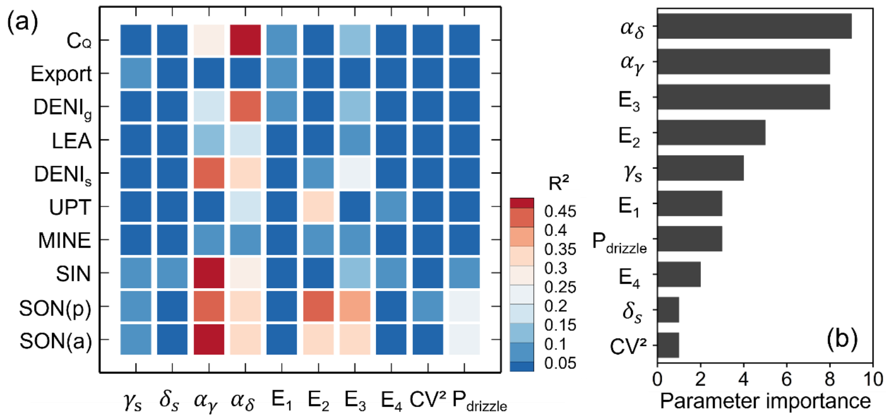

Figure 7. (a) The determination coefficients (R^2) of the linear regressions between the parameters of the rainfall generator and in-stream nitrate concentration (C_Q), N loads, and fluxes. (b) The importance of the parameters influencing the N dynamics.

Storm duration

The parameter α_γ determines how the average storm duration is distributed over the course of a year (Figure 8a). Generally, larger α_γ values represent that storms with longer duration are more likely to occur in mid-year, when ET is high and the inter-storm duration is longer (yellow zone in Figure 8e). This pattern influences not only the drying and rewetting cycles in summer time, but it also supplies more water in the period thereby leading to an overall wet year (e.g., year 2007, α_γ=1.764). The decrease of α_γ causes that storms with longer durations are shifted towards the beginning / end of the year (blue zone in Figure 8e), so that the year becomes drier (e.g., year 2018, α_γ=0.55).

Results suggest that the storm duration distribution during a year can significantly affect the transformation and transport of N. Lower SON load (Figure 8a), but higher SIN

https://doi.org/10.5194/egusphere-2025-676
Preprint. Discussion started: 25 March 2025

load (Figure 8b), can be observed when storms with longer duration occur mid-year. This is due to the fact that the wetter conditions in the catchment can promote the mineralization of SON into SIN, especially for warm periods when mineralization is significantly constrained by soil moisture rather than by temperature. The wetter condition associated with larger α_γ increase the leaching flux of SIN from soil into groundwater (Figure 8c), thereby increasing the average C_Q (Figure 8d). When storms with shorter duration occur mid-year, the transformation and transport of N are subject to retardation.

https://doi.org/10.5194/egusphere-2025-676
Preprint. Discussion started: 25 March 2025

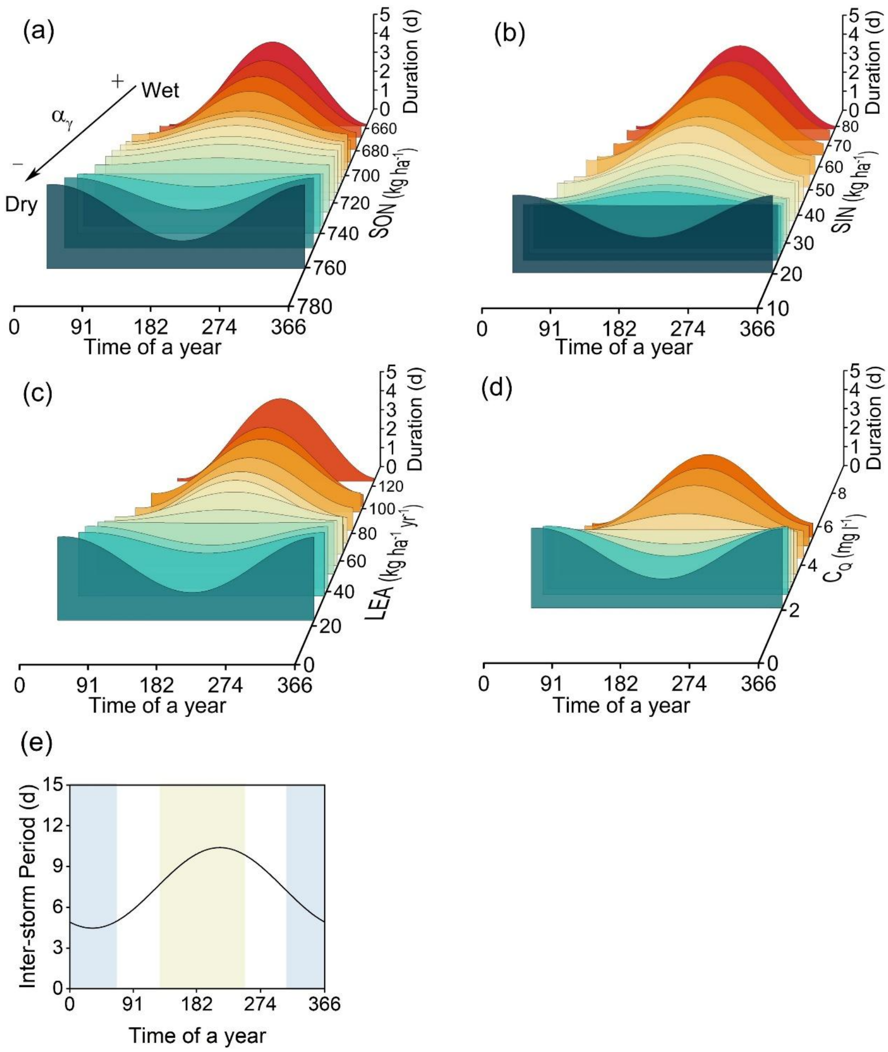

Figure 8. The effect of varied average storm duration distributions over the course of a year on (a) SON load, (b) SIN load, (c) leaching flux, and (d) in-stream nitrate concentration (C_Q). (e) The monthly average inter-storm period over the course of a year (kept constant when α_γ varies). As α_γ values decrease, storms with longer durations shift gradually from the period with high ET and longer inter-storm periods (yellow zone) to the period with low ET and shorter inter-storm periods (blue zone).

Inter-storm duration

α_δ regulates the variation of monthly average inter-storm periods throughout the

https://doi.org/10.5194/egusphere-2025-676
Preprint. Discussion started: 25 March 2025

course of a year (Figure 9a). Large α_δ values imply that long inter-storm durations are more likely to cluster in the middle of the year, which is associated with longer storm durations (blue zone, Figure 9e), while short inter-storm durations occur at the beginning / end of the year, associated with shorter storm durations (yellow zone, Figure 9e). This forms a "wet-dry-wet" climate pattern which promotes the accumulation of SON in the soil (Figure 9a), but reduces the SIN load (Figure 9b), the leaching flux (Figure 9c), and the C_Q (Figure 9d). However, when α_δ decreases, long inter-storm periods are shifted to the beginning / end of the year when the storm durations are short (yellow zone, Figure 9e), forming a "dry-wet-dry" climate pattern over a year. Such a climate pattern results in a lower SON load, but a higher SIN load. This is because wet and warm conditions in the middle of the year promote the mineralization of SON accumulated in the previous season. Consequently, a high leaching flux and high C_Q are also observed.

https://doi.org/10.5194/egusphere-2025-676
Preprint. Discussion started: 25 March 2025

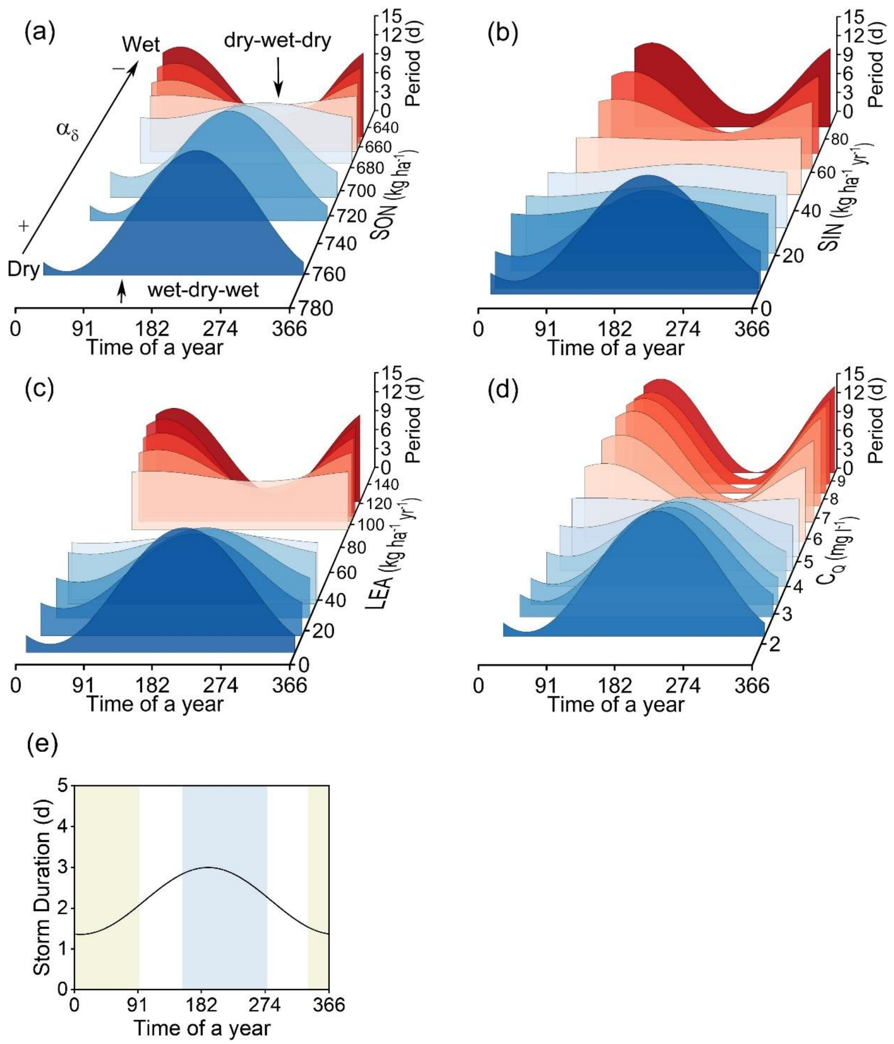

Figure 9. The effect of varied average inter-storm period distributions over the course of a year on (a) SON load, (b) SIN load, (c) leaching flux, and (d) in-stream nitrate concentration (C_Q). (e) The monthly average storm duration over the course of a year (kept constant when α_δ varies). As α_δ values decrease, inter-storms with longer periods shift gradually from the period with longer storm durations (blue zone) to the period with shorter storm durations (yellow zone).

Average Storm Intensity

Figure 10 depicts the responses of SON, SIN, plant uptake, leaching, and C_Q to the

https://doi.org/10.5194/egusphere-2025-676
Preprint. Discussion started: 25 March 2025

average rainfall intensity of the four seasons (E_1, E_2, E_3, and E_4). Basically, increased rainfall intensity creates a more humid catchment, intensifying the biogeochemical processes (e.g., mineralization, plant-uptake). According to the slope of the linear relationship (k), it is suggested that the increase of the rainfall intensity of the second and third seasons (E_2 and E_3) can significantly reduce the SON load (Figure 10b_1 & 10c_1). Rainfall intensity in the first and last seasons (E_1 and E_4) has hardly an effect on the SON loads and fluxes (Figure 10a_1 & 10d_1), probably because the mineralization of SON is more restrained by the low temperature in these seasons. As the only sink of SON, SIN load should theoretically increase with the increase of E_2 and E_3, but a relatively stronger response of SIN just occurs in the third season (Figure 10c_2). A significant increase in the plant-uptake flux, concurrent with the increase of rainfall intensity, is only observed in the second season when plant growth occurs (Figure 10b_3). It follows that sufficient moisture contributes to intense absorption of nutrients by vegetation, but just in the growing season. It can be inferred that extensive plant uptake inhibits the response of SIN to the average rainfall intensity in the second season (Figure 10b_2). In addition, leaching (Figure 10c_4) and denitrification fluxes (in soil, Figure 10c_5) increase with the average storm intensity in the third season as well. The response of the denitrification flux in groundwater to the change of average rainfall intensity exhibits an obvious increase in the third season (Figure 10c_6), as well as a slight decrease in the first season (Figure 10a_6). Finally, note that a change of the average rainfall intensity only causes a minor increase or decrease of C_Q in the first and

https://doi.org/10.5194/egusphere-2025-676
Preprint. Discussion started: 25 March 2025

555 third season (Figure 10a7 & c7), respectively.

556 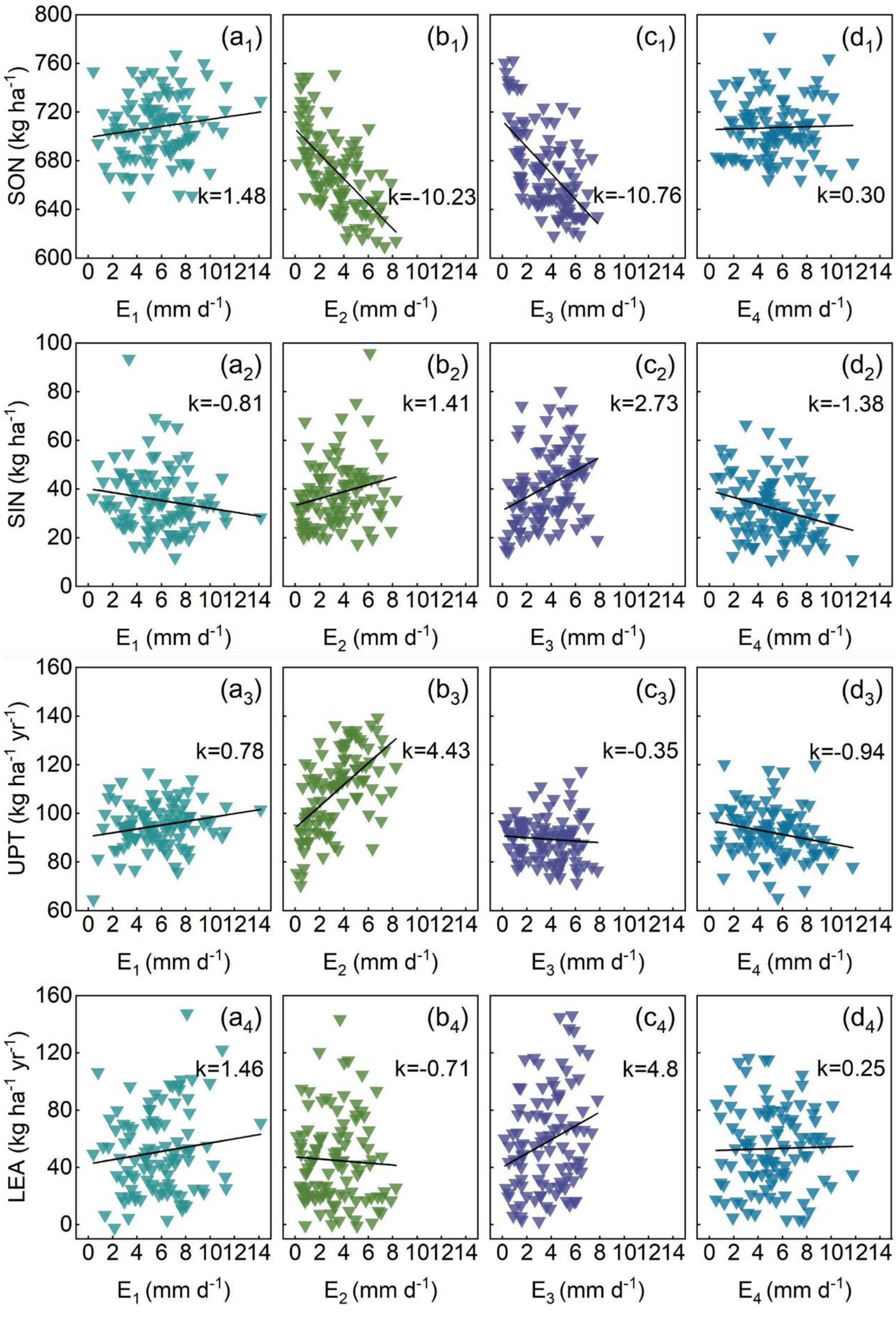

https://doi.org/10.5194/egusphere-2025-676
Preprint. Discussion started: 25 March 2025

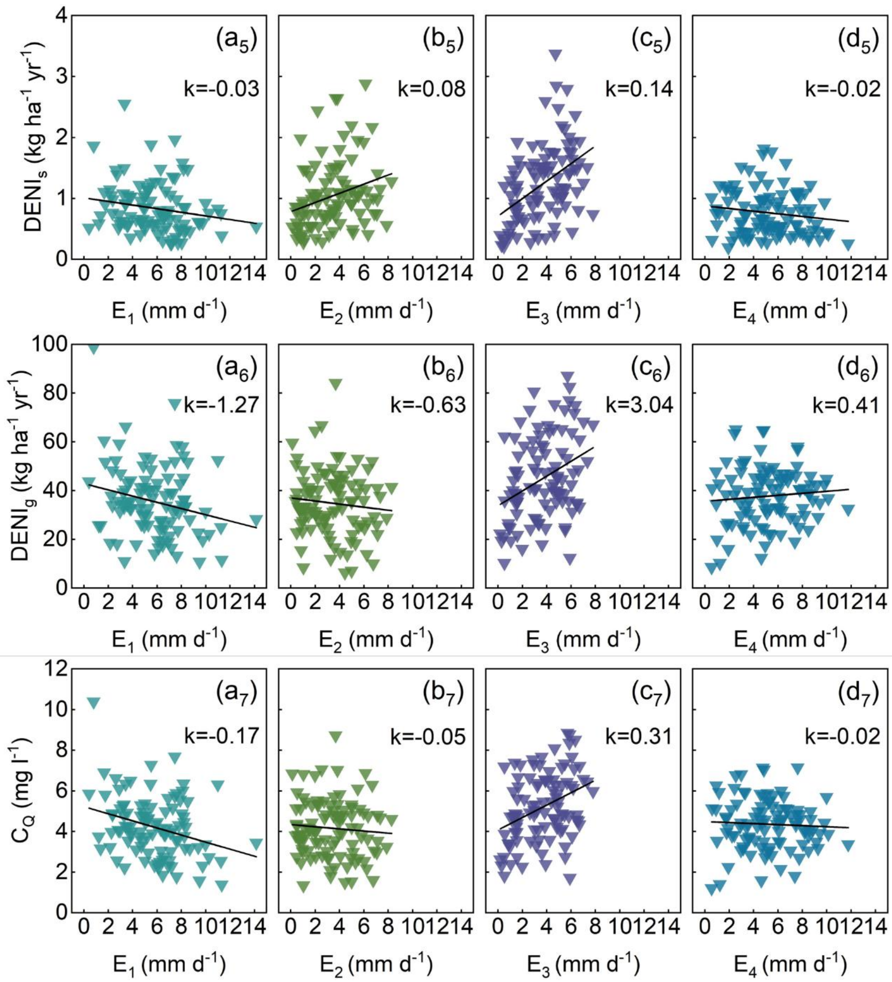

Figure 10. The responses of soil nitrogen loads (SON & SIN), plant uptake and leaching fluxes as well as in-stream nitrate concentration (C_Q) to the average rainfall intensity of the four seasons (E_1, E_2, E_3, and E_4). The symbol and magnitude of the slopes of these linear relationships (k) represent the direction and the intensity of response of N dynamics to the variations in average rainfall intensity, respectively.

5 Discussion

5.1 Increased rainfalls prompt N dynamics

The comparison of C_Q, N loads and N fluxes among the four scenarios of the inter-

https://doi.org/10.5194/egusphere-2025-676
Preprint. Discussion started: 25 March 2025

annual rainfall variability reveals its effect on N dynamics. Mineralization, as the unique process of the transformation from SON to SIN, is impacted by soil wetness and temperatures. With the same soil temperatures assumed for all the scenarios, the average level of mineralization corresponds to the annual wetness conditions. In WY, the mineralization is increased. In contrast, the low mineralization in DY (EDY) leads to the accumulation of SON. Apart from mineralization, the biogeochemical processes relative to SIN, including plant uptake, denitrification, and leaching, are all influenced by soil moisture as well [Yang et al., 2022; Yang et al., 2021]. Their average levels decrease with decreasing wetness conditions from WY, via NY, to DY. In addition, the transport of DIN relies on groundwater discharge and subsurface flow paths. Increased discharge due to changes in precipitation may flush out more nitrogen to surface water bodies [Mitchell et al., 1996; Creed and Band, 1998] by activating shallow preferential flow paths with short transit times [Yang et al., 2018]. Thus, the changes of nitrogen export and C_Q are consistent with the change of wetness conditions between WY, NY, and DY as well. It can be concluded that high annual precipitation amounts can enhance the transformation and transport of nitrogen while low annual precipitation amounts are more conducive for N to be retained in the catchment. Our simulation results echo previous findings that N retention is influenced by changes in precipitation [Dumont et al., 2005; Howarth et al., 2006].

https://doi.org/10.5194/egusphere-2025-676
Preprint. Discussion started: 25 March 2025

5.2 Stream water quality deteriorates during extreme droughts

In the EDY scenario, when the vegetation suffers from drought stress, SIN remarkably accumulates in soil [RIVM, 2021; Winter et al., 2023]. This is because in general plant uptake is the major sink for SIN [Yang et al., 2021; Zhou et al., 2022; Wang et al., 2023]. Due to the accumulation of SIN, denitrification and leaching in the EDY scenario are higher than those of the DY scenario as well. Subsequently, N export to the stream during the EDY scenario is higher than that during the DY scenario, even though the stream discharge is the same (Figure 11). This causes the in-stream nitrate concentration for the EDY scenario to be as high as that of the WY scenario.

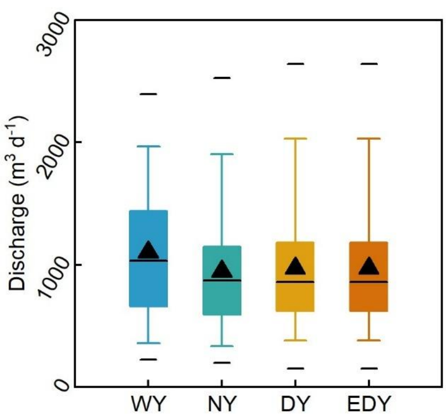

Figure 11. The simulated discharge for the scenarios of WY, NY, DY, and EDY.

During the 2018-2019 drought in central Europe, the observed peaks of in-stream nitrate concentration at a mesoscale catchment in central Germany were significantly higher than previous (Figure 12). Based on the data-driven analysis, Winter et al. [2023] indicated that nitrate loads in the 2018-2019 drought were up to 73% higher than the

https://doi.org/10.5194/egusphere-2025-676
Preprint. Discussion started: 25 March 2025

long-term averaged loads. They demonstrated that such an increase was attributed to decreased plant uptake and subsequent flushing of accumulated nitrogen during the rewetting period. Our results confirmed their findings that reduced plant uptake in extreme droughts causes C_Q to increase (Figure 4(b4)), which suggests that vegetation plays a vital role in the increased risk of N pollution during extreme droughts. Thus, when vegetation suffers from drought stress, the N retention capacity can decline severely.

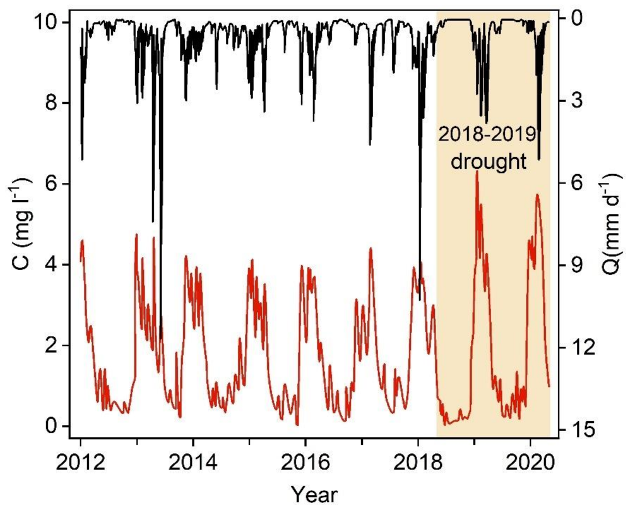

Figure 12. Measured daily averaged nitrate concentrations (C, red line) and discharge (Q, black line) in the nearby Upper Selke catchment in central Germany [Winter et al., 2023]. The yellow area marks the 2018-2019 drought occurring across central Europe.

5.3 The distribution of storm durations controls the N loads

Our study indicates that the wet / dry conditions in the middle of a year are key to the transformation and transport of N throughout the whole year. The combination of longer storms and longer inter-storm periods mid-year represents an aspect of extreme climate

https://doi.org/10.5194/egusphere-2025-676
Preprint. Discussion started: 25 March 2025

events that finds that intense rainfalls alternate with drought periods [Zhang et al., 2024]. Without temperature limitations, alternating longer storm durations and longer inter-storm periods increase the extensive transformation of SON, which is consistent with the results of laboratory studies that mineralization increased after successive drying and rewetting cycles in soils [Cabrera, 1993]. It is concluded thereby that drying-rewetting events induce the prominent changes in N dynamics [Fierer & Schimel, 2002]. However, the drier conditions induced by shortened storm durations and longer inter-storm periods in mid-year cause the accumulation of SON, which is consistent with the finding by Zhou et al. [2022] that droughts in the warm season contribute to nitrogen retention in catchments. Thus, the distribution of storm duration within a year can significantly affect N loads in a catchment.

5.4 The distribution of inter-storm periods changes stream water quality

Different dry-wet patterns over the course of a year have an impact on N dynamics as well, with a specifically intense focus on in-stream nitrate concentration. In the “dry-wet-dry” pattern, the accumulation of SON during the previous dry season is transformed and transported during the subsequent wetting period, which leads to higher C_Q. In the 2018-2019 drought, accumulated N loads were flushed during the rewetting period and thereby caused elevated nitrate loads (Figure 12). In the “wet-dry-wet” pattern, wetter conditions but low temperatures in the beginning of the year and

https://doi.org/10.5194/egusphere-2025-676
Preprint. Discussion started: 25 March 2025

warm droughts in mid-year both cause SON loads to accumulate throughout the entire year and C_Q to decrease in general. The result that reduced C_Q may be attributed to limited terrestrial export loading was proven by Zhou et al. [2022]. In summary, the distribution of inter-storm periods during a year can cause noticeable variations in water quality in terms of nitrate concentration.

5.5 Average rainfall intensity has only a small effect on stream water quality

Wet conditions caused by high mean rainfall intensities contribute to the transformation of SON to SIN [Knapp and Smith, 2001], if mineralization is not constrained by low temperatures (Equation 1 & 2). The potential plant uptake is subject to the state of vegetation (Equation 6), and the actual plant uptake is further limited by SIN load and soil moisture content (Equation 5) [Yang et al., 2022; Cramer et al., 2009]. Thus, high mean rainfall intensities increase plant absorption of inorganic nitrogen in the growing season. Since plant uptake is the major sink of SIN, SIN flux hardly responds to the variations of mean rainfall intensities in the season of growth. Leaching and denitrification fluxes (in the soil) are determined by SIN load, soil saturation, and groundwater velocity (Equation 3 & 7-9). As a result, the fluxes increase remarkably when the average rainfall intensity in the third season increases. The denitrification efficiency in groundwater depends on transit time. In the first season, increased discharge caused by enhanced rainfall intensity (Figure S2a) accelerates the transport

https://doi.org/10.5194/egusphere-2025-676
Preprint. Discussion started: 25 March 2025

of DIN and thus cuts down the denitrification flux [Wang et al., 2023]. However, due to high ET in the third season, decreased discharge (Figure S2c) can prolong the transit time of DIN and may increase denitrification. It is noteworthy that the unexpectedly weak response of C_Q to the average rainfall intensity may be caused by the fact that high-intensity precipitation events tend to have short durations and yield surface runoff. It is less likely for the extreme precipitation to propagate to the groundwater zone and impact the discharge and nitrate export (see Figure S2 in the supporting information).

On the whole, increased variations in precipitation can alter the transformation and transport of nitrogen [Kane et al., 2008]. The results of the present study can help in managing the water quality of agricultural catchments with prominent rainfall variability and protect aquatic ecosystems during extreme rainfall and droughts in the future. For instance, the formulation of a fertilization scheme for inter-storm periods to avoid flushing in the rewetting periods after droughts. Also, increased fertilization in the wet season of the growing season not only is conducive to vegetation absorption of nutrients, but also does not cause pressure on soil and water bodies.

5.6 Limitations and Outlook

The contribution of high temperatures to extreme droughts has not been considered in the present study. High temperatures induced several remarkable hydrological and agricultural droughts in Central Germany, which even destroyed vegetation activities [Fink et al., 2004; Camenisch et al., 2020; Liu et al., 2020; Schuldt et al., 2022; Winter

https://doi.org/10.5194/egusphere-2025-676
Preprint. Discussion started: 25 March 2025

et al., 2022]. Considering the phenomenon, the present study indicates that vegetation plays a quite significant role in N dynamics only by assuming reduced plant uptake. Apart from that, both mineralization and denitrification are subject to temperature. For instance, the biological activities of denitrifying bacteria are impacted by high temperatures that can cause an increase in denitrification efficiency [Amatya et al., 2009]. Thus, high temperatures can influence the nitrogen retention capacity of catchments. The effect of rising temperatures on water quality and the environment in terms of N dynamics should be investigated in detail.

In the future, the alteration of soil properties caused by rainfall variability should be studied in the model. In the model, precipitation and solute enter the subsurface domain with fixed soil porosity, ignoring the alteration of pores. Abundant microorganisms and animals engage in extensive activities, and massive organic and inorganic matter undergoes biochemical reactions in soil pores, which all change the physical and chemical properties of porous media and thereby impact the process of seepage. These biogeochemical processes are determined by several factors, such as hydrometerological conditions [Ondrasek et al., 2019]. For example, under drying conditions, the activities of microorganisms and animals diminish which is not helpful to the maintenance and improvement of soil structures. The severe deficit of soil moisture causes the destruction of soil aggregates, more micropores replace macropores and even compacted soil forms in the upper layer due to salt clusters, which thereby decreases the porosity. What's more, extreme droughts may cause surface soil to crack,

https://doi.org/10.5194/egusphere-2025-676
Preprint. Discussion started: 25 March 2025

which is adverse to plant growth and root development. Not to mention that changing soil properties caused by complex and extreme climate patterns may have an effect on the biogeochemical activities in soil. Consequently, the clarification of these mechanisms will be conducive to exploring the more realistic response of solute transport in groundwater to extreme rainfall and droughts.

6. Conclusions

In the context of climate change and the frequent occurrence of extreme rainfall and droughts, the study adopted a stochastic rainfall generator (Robinson and Sivapalan, 1997) to explore the effects of inter-annual and intra-annual rainfall variability on N dynamics for the first time in a small agricultural catchment in Central Germany. The main conclusions of this study are:

(1) Higher annual precipitation amounts can enhance the transformation and transport of nitrogen. Lower annual precipitation amounts are conducive to the nitrogen retention capacity. Nonetheless, when vegetation suffers from drought stress, the retention capacity will decline severely. Vegetation plays a vital role in N dynamics under extreme droughts.

(2) Wet / dry conditions determined by the distribution of storm durations within a year can significantly affect N loads within a catchment. Droughts can prompt the accumulation of SON, but a drying-wetting cycle can enhance extensive transformation of SON in the warm season.

https://doi.org/10.5194/egusphere-2025-676
Preprint. Discussion started: 25 March 2025

(3) Different dry-wet patterns formed by the distribution of inter-storm periods during a year can cause noticeable variations in water quality. In-stream nitrate concentration prominently elevates during the rewetting period after the drought.

(4) High mean rainfall intensity contributes to the transformation of N when mineralization is not limited by low temperatures, and to plant absorption of inorganic nitrogen in the growing season. There is merely a small effect on stream water quality.

Overall, the study clarifies the effect of rainfall variability on N dynamics in a small agricultural catchment, which provides theoretical support to formulate fertilization strategies and protect aquatic ecosystems under the context of climate change in the future.

Code availability. All data used in this study are listed in the supporting information and uploaded separately to HydroShare [Wang, 2024].

Author contributions. QW contributed to the conceptualization, methodology, software, formal analysis, visualization, and writing (review and editing). JY contributed to the conceptualization, methodology, formal analysis, and writing (review and editing). IH contributed to the writing (review and editing). TX contributed to the conceptualization and review and editing. CL contributed to the methodology, and review and editing.

Competing interests. The contact author has declared that none of the authors has any competing interests.

Disclaimer. Publisher' note: Copernicus Publications remains neutral with regard to jurisdictional claims in published maps and institutional affiliations.

Acknowledgements. We thank Daniel C. Wilusz for the source code in Python v2.7 of the rainfall generator [Wilusz et al., 2017] and Min Yan and Huiqiang Wu for stimulating discussions.

Financial support. This research was supported by the National Key Research and Development Project, China (JY & CL: 2021YFC3200500), the National Natural Science Foundation of China, China (JY & CL: U2340212, JY: 52009032, TX: 42377046, CL: 51879088), and the Natural Science Foundation of Jiangsu Province, China (CL: BK20190023).

Reference

Acreman, M. C. (1990): A simple model of hourly rainfall for Farnborough, England, Hydrol. Sci. J., 35, 119-148, 1990.

Altermann, M., Mautschke, J. (1970): Ergebnisbericht über quartärgeologische bodenhydrologische Untersuchungen im Gebiet des Schäfertals und Waldbachs bei Siptenfelde. VEB GFE Halle.

Altermann, M., Pretzschel, M., Mautschke, J., Erbe, C. (1977): Zur Kennzeichnung der quartären Deckschichten im Unterharz. Petermanns Geografische Mitteilungen 2/77.

Altermann, M., Steininger, M. (1994): Vom Bodenprofil zum Gebietswasserhaushalt Untersuchungen aus dem Unterharz. Mitteilungen der DBG, 74, 167-170.

Alvarez-Cobelas, M., Angeler, D.G., Sánchez-Carrillo, S. (2008): Export of nitrogen from catchments: a worldwide analysis. Environ. Pollut. 156 (2), 261–269. https://doi.org/10.1016/j.envpol.2008.02.016.

Amatya, I. M., Kansakar, B. R., Tare, V., & Fiksdal, L. (2009): Impact of Temperature on Biological Denitrification Process. Journal of the Institute of Engineering, 7(1), 121–126. https://doi.org/10.3126/jie.v7i1.2070.

https://doi.org/10.5194/egusphere-2025-676
Preprint. Discussion started: 25 March 2025

Anis, M. R., & Rode, M. (2015): Effect of climate change on overland flow generation: A case study in central Germany. Hydrological Processes, 29(11), 2478–2490.

Bach, M., Frede, H.-G. (1998): Agricultural nitrogen, phosphorus and potassium balances in Germany methodology and trends 1970 to 1995. Zeitschrift für Pflanzenernährung und Bodenkunde 161 (4), 385–393. https://doi.org/10.1002/ jpln.1998.3581610406.

Bach, M., Godlinski, F., Greef, J.-M. (2011): Handbuch Berechnung der Stickstoffbilanz für die Landwirtschaft in Deutschland. Jahre 1990–2008, 159.

Ballard, T.C., Sinha, E., Michalak, A.M. (2019): Long-term changes in precipitation and temperature have already impacted nitrogen loading. Environ. Sci. Technol. 53 (9), 5080–5090.

Bauwe. A., Kahle. P., Tiemeyer. B., & Lennartz. B. (2020): Hydrology is the key factor for nitrogen export from tile-drained catchments under consistent land-management. https://doi.org/10.1088/1748-9326/aba580.

BDF (Bund Deutscher Forstleute). (2019): Der Wald ist in Gefahr Die Politik muss handeln. Pressemitteilung: Marshallplan f ü r den Wald. 29.03.2019 https://www.bdf-online.de/fileadmin/user_upload/www_bdf-online_de/pdf/2019/19-05_Wald_in_Gefahr_-_Marshallplan_fuer_den_Wald_noetig.pdf.

Black, E. (2023): Global change in agricultural flash drought over the 21st century. Adv. Atmos. Sci., https://doi. org/10.1007/s00376-023-2366-5.

Borchardt, D. (1981): Geoökologische Erkundung und hydrologische Analyse von Kleineinzugsgebieten des unteren Mittelgebirgsbereichs, dargestellt am Beispiel von Experimentalgebieten der oberen Selke/Harz. Petermanns Geografische Mitteilungen 4/82.

Cabrera, M. (1993): Modeling the flush of nitrogen mineralization caused by drying and rewetting soils. Soil Science Society of America Journal 57: 63-66.

Camenisch, C., Bräzdil, R., Kiss, A., Pfister, C., Wetter, O., Rohr, C., Contino, A., & Retsö, D. (2020): Extreme heat and drought in 1473 and their impacts in Europe in the context of the early 1470s. Regional Environmental Change, 20, 19.

Chow,V. T., D. R. Maidment, and L. W. Mays. (1988): Applied Hydrology, 572 pp., McGraw-Hill, New York.

Ciais, P., et al. (2005): Europe-wide reduction in primary productivity caused by the heat and drought in 2003. Nature 437, 529–533.

Cramer, M. D., Hawkins, H.-J., and Verboom, G. A. (2009): The importance of nutritional regulation of plant water flux, Oecologia, 161, 15–24, https://doi.org/10.1007/s00442-009-1364-3.

Dai, A. (2013): Increasing drought under global warming in observations and models. Nat. Clim. Change 3, 52–58.

https://doi.org/10.5194/egusphere-2025-676
Preprint. Discussion started: 25 March 2025

Delpla, I., Jung, A.-V., Baures, E., Clement, M., & Thomas, O. (2009): Impacts of climate change on surface water quality in relation to drinking water production. Environment International, 35(8), 1225–1233. https://doi.org/10.1016/j.envint.2009.07.001.

Doherty, J. E., & Hunt, R. J. (2010): Approaches to highly parameterized inversion-a guide to using pest for groundwater-model calibration (Tech. rep 2010-5211). Reston, VA: US Geological Survey.

Creed IF, Band LE. (1998): Export of nitrogen from catchments within a temperate forest: evidence for a unifying mechanism regulated by variable source area dynamics. Water Resources Research 34: 3105-3120.

Dumont, E. L., Harrison, J. A., Kroeze, C., Bakker, E. J., Seitzinger, S. P. (2005): Global distribution and sources of dissolved inorganic nitrogen export to the coastal zone: results from a spatially explicit, global model. Global Biogeochemical Cycles 19: GB4S02, DOI: 10.1029/2005GB002488.

Dupas, R., Musolff, A., Jawitz, J.W., Rao, P. S. C., Jäger, C. G., Fleckenstein, J. H., Rode, M., Borchardt, D. (2017): Carbon and nutrient export regimes from headwater catchments to downstream reaches. Biogeosciences 14 (18), 4391–4407. https://doi.org/10.5194/bg- 14-4391-2017.

Fink, A. H., et al. (2004): Te 2003 European summer heatwaves and drought–synoptic diagnosis and impacts. Weather. 59, 209–216.

Fischer, E., Knutti, R. (2014): Detection of spatially aggregated changes in temperature and precipitation extremes. Geophys. Res. Lett. 41, 547–554.

Fierer, N., Schimel, J. P. (2002): Effects of drying-rewetting frequency on soil carbon and nitrogen transformations. Soil Biology & Biochemistry 34:777-787.

Geris, J., Comtea, J. C., Franchib, F., Petrosc, A., Tirivarombob, S., Selepeng, A., Villholth, K. (2022): Surface water-groundwater interactions and local land use control water quality impacts of extreme rainfall and flooding in a vulnerable semi-arid region of Sub-Saharan Africa. Journal of Hydrology S0022-1694(22)00409-7. https://doi.org/10.1016/j.jhydrol.2022.127834.

Graeff, T., Zehe, E., Reusser, D., Lück, E., Schröder, B., Wenk, G., John, H., Bronstert, A. (2009): Process identification through rejection of model structures in a mid-mountainous rural catchment: Observations of rainfall-runoff response, geophysical conditions and model inter-comparison. Hydrological Processes, 23(5), 702–718. https://doi.org/10.1002/hyp.7171.

Haag, D., Kaupenjohann, M. (2001): Landscape fate of nitrate fluxes and emissions in central Europe: a critical review of concepts, data, and models for transport and retention. Agric. Ecosyst. Environ. 86 (1), 1–21.

https://doi.org/10.5194/egusphere-2025-676
Preprint. Discussion started: 25 March 2025

Hanel, M., Rakovec, O., Markonis, Y., Maca, P., Samaniego, L., Kysely, J., & Kumar, R. (2018): Revisiting the recent European droughts from a long-term perspective. Scientific Reports, 8, 1–11.

Hari, V., Rakovec, O., Markonis, Y., Hanel, M., & Kumar, R. (2020): Increased future occurrences of the exceptional 2018–2019 Central European drought under global warming. Scientific Reports, 10(1), 1–10. https://doi.org/10.1038/s41598-020-688729.

Hesse, C., Krysanova, V. (2016): Modeling climate and management change impacts on water quality and in-stream processes in the Elbe River Basin. Water 8 (2), 40.

Howarth, R. W., Swaney, D. P., Boyer, E. W., Marino, R., Jaworski, N., Goodale, C. (2006): The influence of climate on average nitrogen export from large watersheds in the Northeastern United States. Biogeochemistry 79: 163-186.

Huff, F. A. (1967): Time distribution of rainfall in heavy storms, Water Resource. Res., 3, 1007-1018.

Ionita, M., Tallaksen, L. M., Kingston, D. G., Stagge, J. H., Laaha, G., Van Lanen, H. A. J., Scholz, P., Chelcea, S. M., Haslinger, K. (2017): The European 2015 drought from a climatological perspective. Hydrol. Earth Syst. Sci. 21, 1397–1419.

IPCC. (2007): Climate change 2007: the physical science basis, vol 1009. Cambridge University Press, Cambridge.

Kane, E., Betts, E., Burgin, A. J., Clilverd, H., Crenshaw, C. L., Fellman, J., Myers-Smith, I., O'donnell, J., Sobota, D. J., Van Verseveld, W. J. (2008): Precipitation control over inorganic nitrogen import–export budgets across watersheds: a synthesis of longterm ecological research. Ecohydrology 1, 105–117.

Knapp, A. K., Smith, M. D. (2001): Variation among biomes in temporal dynamics of aboveground primary production. Science 291: 481-484.

Laaha, G., et al. (2017): The European 2015 drought from a hydrological perspective. Hydrol. Earth Syst. Sci., 21, 3001–3024. https://doi.org/10.5194/hess-21-3001-2017.

Leitner, S., Dirnböck, T., Kobler, J., Zechmeister-Boltenstern, S. (2020): Legacy effects of drought on nitrate leaching in a temperate mixed forest on karst. Journal of Environmental Management 262, 110338.

Lindström, G., Pers, C., Rosberg, J., Strömqvist, J., and Arheimer, B. (2010): Development and testing of the HYPE (Hydrological Predictions for the Environment) water quality model for different spatial scales. Hydrology Research, 41.3 ‐ 4.

Liu, E., Mei, X., Gong, D., Yan, C., Zhuang, Y. (2010): Effects of drought on N absorption and utilization in winter wheat at different developmental stages. Chinese Journal of Plant Ecology, 34 (5): 555–562.

https://doi.org/10.5194/egusphere-2025-676
Preprint. Discussion started: 25 March 2025

Liu, X., He, B., Guo, L., Huang, L., & Chen, D. (2020): Similarities and differences in the mechanisms causing the European summer heatwaves in 2003, 2010, and 2018. Earth's Future in press.

Markonis, Y., Kumar, R., Hanel, M., Rakovec, O., Máca, P., AghaKouchak, A. (2021): The rise of compound warm-season droughts in Europe. Science Advances 7(6):eabb9668. DOI: 10.1126/sciadv.abb9668

Min, S. K., Zhang, X., Zwiers, F. W., & Hegerl, G. C. (2011): Human contribution to more-intense precipitation extremes. Nature 470, 378–381.

Mitchell, M. J., Driscoll, C. T., KahI, J. S., Likens, G. E., Murdoch, P. S., Pardo, L. H. (1996): Climatic control of nitrate loss from forested watersheds in the northeast United States. Environmental Science & Technology 30:2609-2612.

Mosley, L. M. (2015): Drought impacts on the water quality of freshwater systems; review and integration. Earth Sci. Rev. 140, 203–214.

Nguyen, T. V., Kumar, R., Lutz, S. R., Musolff, A., Yang, J., & Fleckenstein, J. H. (2021): Modeling nitrate export from a mesoscale catchment using storage selection functions. Water Resource. Res., 56, e2020WR028490. 10.1029/2020WR028490.

Ondrasek, G., Begić, B. H., Zovko, M., Filipović, L., Meriño-Gergichevich, C., Savić, R., Rengel, Z. (2019): Biogeochemistry of soil organic matter in agroecosystems & environmental implications, Science of The Total Environment, Volume 658, Pages 1559-1573, ISSN 0048-9697, https://doi.org/10.1016/j.scitotenv.2018.12.243.

Orth, R., Vogel, M. M., Luterbacher, J., Pfister, C., & Seneviratne, S. I. (2016): Did European temperatures in 1540 exceed present-day records. Environmental Research Letters, 11, 1–10.

Otkin, J., Svoboda, M., Hunt, E. D., Ford, T. W., Anderson, M., Hain, C., & Basara, J. B. (2018): Flash droughts: A review and assessment of the challenges imposed by rapid onset droughts in the United States. Bull. Amer. Meteor. Soc., 99, 911–919, https://doi.org/10.1175/BAMS-D-17-0149.1.

O'Gorman, P. A., & Schneider, T. (2009): The physical basis for increases in precipitation extremes in simulations of 21st-century climate change. Proc. Natl Acad. Sci. 106, 14773–14777.

Pall, P., et al. (2011): Anthropogenic greenhouse gas contribution to flood risk in England and Wales in autumn 2000. Nature 470, 382–385.

Pendergrass, A. G., Knutti, R., Lehner, F., Deser, C., & Sanderson, B. M. (2017): Precipitation variability increases in a warmer climate. Sci. Rep. 7, 17966.

Robinson, J., & Sivapalan, M. (1997): Temporal scales and hydrological regimes: Implications for flood frequency scaling. Water Resources Research, VOL. 33, NO. 12, Pages 2981-2999. https://doi.org/10.1029/97WR01964.

https://doi.org/10.5194/egusphere-2025-676
Preprint. Discussion started: 25 March 2025

Schär, C., Vidale, P. L., Lüthi, D., Frei, C., Häberli, C., Liniger, M. A., & Appenzeller, C. (2004): The role of increasing temperature variability in European summer heatwaves. Nature, 427, 332–336.

Schuldt, B., Buras, A., Arend, M., Vitasse, Y., Beierkuhnlein, C., Damm, A., et al. (2020): A first assessment of the impact of the extreme 2018 summer drought on Central European forests. Basic and Applied Ecology, 45, 86–103. https://doi.org/10.1016/j.baae.2020.04.003

Spinoni, J., Vogt, J.V., Naumann, G., Barbosa, P., Dosio, A. (2018): Will drought events become more frequent and severe in Europe? Int. J. Climatol. 38 (4), 1718–1736.

Stahl, K., Kohn, I., Blauhut, V., Urquijo, J., De Stefano, L., Acácio, V., Dias, S., Stagge, J. H., Tallaksen, L. M., Kampragou, E., Van Loon, A. F., Barker, L. J., Melsen, L. A., Bifulco, C., Musolino, D., de Carli, A., Massarutto, A., Assimacopoulos, D., & Van Lanen, H. A. J. (2016): Impacts of European drought events: insights from an international database of text-based reports, Nat. Hazards Earth Syst. Sci., 16, 801–819, doi:10.5194/nhess-16-8012016.

Therrien, R., McLaren, Sudicky, R. E., & Panday, S. (2010): Hydrogeosphere: A three-dimensional numerical model describing fully-integrated subsurface and surface flow and solute transport, Groundwater Simulations Group. Waterloo, ON: University of Waterloo.

Thieken, A. H., Kienzler, S., Kreibich, H., Kuhlicke, C., Kunz, M., Mühr, B., Müller, M., Otto, A., Petrow, T., Pisi, S., & Schröter, K. (2016): Review of the flood risk management system in Germany after the major flood in 2013. Ecology and Society 21(2):51. http://dx.doi.org/10.5751/ES-08547-210251.

Trenberth, K. E. (2011): Changes in precipitation with climate change. Climate. Res. 47, 123–138.

Ulbrich, U., Brücher, T., Fink, A., Leckebusch, G. C., Krüger, A., & Pinto, J. G. (2003): The central European floods of August 2002: Part 1 - Rainfall periods and flood

development. Weather 58(10):371-377. DOI: 10.1256/wea.61.03A.

Van Lanen, H. A. J., et al. (2016): Hydrology needed to manage droughts: the 2015 European case. HYDROLOGICAL PROCESSES Hydrol. Process. 30, 3097–3104.

Van Meter, K. J., Basu, N. B., Van Cappellen, P. (2017): Two centuries of nitrogen dynamics: Legacy sources and sinks in the Mississippi and susquehanna river basins. Global Biogeochem. Cycles 31 (1), 2–23. https://doi.org/10.1002/2016GB005498.

Vitousek, P. M., et al. (2009): Nutrient imbalances in agricultural development. Science, 324(5934), 1519–1520. 10.1126/science.1170261.

Voit, P., & Heistermann, M. (2024): A downward-counterfactual analysis of flash floods in Germany. Nat. Hazards Earth Syst. Sci., 24, 2147–2164. https://doi.org/10.5194/nhess-24-2147-2024.

Wang, Q. (2024): DS2024-1WQ, HydroShare, http://www.hydroshare.org/resource/1199c12ae64447bd87d5c005a11e984c.

Wang, Q., Yang, J., Heidbüchel, I., Yu, X., Lu, C. (2023): Flow paths and wetness conditions explain spatiotemporal variation of nitrogen retention for a temperate, humid catchment. Journal of Hydrology 625(2):130024. DOI: 10.1016/j.jhydrol.2023.130024.

Watmough, S. A., Aherne, C. E. J., Dillon, P. J. (2004): Climate Effects on Stream Nitrate Concentrations at 16 Forested Catchments in South Central Ontario. Environmental Science and Technology 38(8):2383-8. DOI: 10.1021/es035126l.

Wegren, S. K. (2010): Food Security and Russia's 2010 Drought. Eurasian Geogr. Econ., https://doi.org/10.2747/1539-7216.52.1.140, 2011.

Whitehead, P.G., Wilby, R. L., Battarbee, R. W., Kernan, M., Wade, A. J. (2009): A review of the potential impacts of climate change on surface water quality. Hydrol. Sci. J. 54 (1), 101–123.

Williams, A. P., Seager, R., Abatzoglou, J. T., Cook, B. I., Smerdon, J. E., Cook, E. R. (2015): Contribution of anthropogenic warming to California drought during 2012–2014. Geophysical Research Letters 42(16):6819-6828. DOI: 10.1002/2015GL064924.

Wilusz, D. C., Harman, C. J., & Ball, W. P. (2017): Sensitivity of catchment transit times to rainfall variability under present and future climates. Water Resources Research, 53, 10,231–10,256. https://doi.org/10.1002/ 2017WR020894.

Winter, C., Nguyen, T., Musolff, A., Lutz, S., Rode, M., Kumar, R., Fleckenstein, J. (2023): Droughts can reduce the nitrogen retention capacity of catchments. January 2023, Hydrology and Earth System Sciences 27(1):303-318. https://doi.org/10.5194/hess-27-303-2023.

Winter, C., Müller, S., Kattenborn, T., Stahl, K., Szillat, K., Weiler, M., Schnabel, F. (2024): Forest dieback in drinking water protection areas – a hidden threat to water quality.

Wollschläger, U., Attinger, S., Borchardt, D., Brauns, M., Cuntz, M., Dietrich, P. (2016): The bode hydrological observatory: A platform for integrated, interdisciplinary hydro-ecological research within the Tereno Harz/central German lowland observatory. Environmental Earth Sciences, 76(1), 29. https://doi.org/10.1007/s12665-016-6327-5.

Yang, J., Graf, T., & Ptak, T. (2015): Impact of climate change on freshwater resources in a heterogeneous coastal aquifer of Bremerhaven, Germany: A three-dimensional modeling study. Journal of Contaminant Hydrology, 177, 107–121.

Yang J., Heidbüchel, I., Musolff, A., Reinstorf, F., and Fleckenstein. J. H. (2018): Exploring the dynamics of transit times and subsurface mixing in a small agricultural catchment. Water Resources Research, 54. https://doi.org/ 10.1002/2017WR021896.

https://doi.org/10.5194/egusphere-2025-676
Preprint. Discussion started: 25 March 2025

Yang J., Heidbüchel, I., Musolff, A., Xie, Y., Lu, C., Fleckenstein. J. H. (2021): Using nitrate as a tracer to constrain age selection preferences in catchments with strong seasonality. Journal of Hydrology 603 (2021) 126889. https://doi.org/10.1016/j.jhydrol.2021.126889.

Yang, X., Rode, M., Jomaa, S., Merbach, I., Tetzlaff, D., Soulsby, C., & Borchardt, D. (2022): Functional multi-scale integration of agricultural nitrogen-budgets into catchment water quality modeling. Geophysical Research Letters, 49, e2021GL096833. https://doi.org/10.1029/2021GL096833.

Zhang, W., et al. (2021): Increasing precipitation variability on daily-to-multiyear time scales in a warmer world. Sci. Adv. 7, eabf8021.

Zhang, W., Zhou, T., Wu, P. (2024): Anthropogenic amplification of precipitation variability over the past century. Science 385, 427–432. https://www.science.org/doi/10.1126/science.adp0212.

Zhou, X., Jomaa, S., Yang, X., Merz, R., Wang, Y., Rode, M. (2022): Exploring the relations between sequential droughts and stream nitrogen dynamics in central Germany through catchment-scale mechanistic modelling. Journal of Hydrology 614 (2022) 128615. https://doi.org/10.1016/j.jhydrol.2022.128615.

Zwolsman, J. J. G., van Bokhoven, A. J. (2007): Impact of summer droughts on water quality of the Rhine River – a preview of climate change? Water Sci. Technol. 56 (4), 45–55.